Developmental Biology 411 (2016) 301–313

Contents lists available at ScienceDirect

Developmental Biology

journal homepage: www.elsevier.com/locate/developmentalbiology

Developmental transcriptomics in Atlantic haddock: Illuminating pattern formation and organogenesis in non-model vertebrates

Elin Sørhus [a,b,*], John P. Incardona [c], Tomasz Furmanek [a], Sissel Jentoft [b,d], Sonnich Meier [a], Rolf B. Edvardsen [a]

[a] Institute of Marine Research, P.O. Box 1870, Nordnes, 5817 Bergen, Norway
[b] Centre for Ecological and Evolutionary Synthesis (CEES), University of Oslo, P.O. Box 1066, Blindern, NO-0316 Oslo, Norway
[c] Environmental and Fisheries Science Division, Northwest Fisheries Science Center, National Marine Fisheries Service, NOAA, 2725 Montlake Blvd. E., Seattle, WA 98112, United States
[d] Department of Natural Sciences, University of Agder, 4604 Kristiansand, Norway

ARTICLE INFO

Article history:
Received 5 November 2015
Received in revised form
10 February 2016
Accepted 10 February 2016
Available online 12 February 2016

ABSTRACT

Gadiforms such as Atlantic haddock comprise some of the world's most economically important fisheries. Understanding the early life history of these fish is a prerequisite for predicting effects of a changing environment and increased human activities. Robust assessment of the effects of environmental impacts on the embryos of non-model vertebrates is hampered by a lack of molecular resources and detailed knowledge regarding the regulation of genes and pathways in early development. Here we used mRNA sequencing to link transcriptional changes to developmental processes in haddock, specifically, pattern formation and organogenesis. Temporal expression of key developmental genes was tightly anchored to either the appearance of visible structures or cellular processes characterised in model organisms. These findings demonstrate the high potential of developmental transcriptomics as an analytical tool for improved understanding of pathophysiological mechanisms leading to abnormal development in any vertebrate.

1. Introduction

Developmental genetics in model organisms has provided the basis for major advances in other areas of biology and medicine. In contrast, a major challenge for a detailed understanding of development in non-model organisms is a lack of genetic tools. In addition, embryology in general is highly dependent on visual (i.e., microscopic) analysis of structure. Indeed, the exquisite translucency of fish embryos in particular has made zebrafish one of the best model systems for visualising cellular and structural aspects of development in real time in live embryos, or in fixed specimens using techniques such as whole mount in situ hybridisation or antibody labelling.

A quandary arises in studies with non-model fish (and other taxa) in which both the lack of molecular and cellular tools and limited access to embryos precludes the usual quantitative approaches to visual analyses of development achievable with models such as zebrafish. Genomics coupled with transcriptome profiling through deep-sequencing has the potential to overcome this roadblock. Anchoring the timing and abundance of mRNA levels for suites of genes to measureable phenotypes could provide a proxy measure of the development of specific structures in the absence of visual information. For work in non-model species, our long term goal is to determine whether quantitative measures of gene expression can provide information on the status of structures in embryos that are available in very limited numbers. This approach has practical applications for assessing the development of embryos in field samples from environmental studies, for example. The need for this approach is highlighted by studies on the environmental impacts of oil spills in particular, which are likely to affect a large number and diversity of species that simply are not amenable to cellular and molecular techniques associated with model species (e.g., Edmunds et al., in press; Incardona et al., 2014; Jung et al., 2015).

Here we focus on Atlantic haddock, *Melanogrammus aeglefinus* (family Gadidae), as a candidate for phenotypic anchoring of a developmental transcriptome. Atlantic haddock is a commercially important fish distributed throughout the North Atlantic. The combined annual landings and value within the last decade are reported to be in the range of 130,000 metric tons and $200,000,000, respectively, for North America and Northern Europe. In Norway, the areas surrounding Lofoten and Vesterålen are

* Corresponding author at: Institute of Marine Research, P.O. Box 1870, Nordnes, 5817 Bergen, Norway.
E-mail address: Elin.sorhus@imr.no (E. Sørhus).

http://dx.doi.org/10.1016/j.ydbio.2016.02.012
0012-1606/

considered to be the main spawning grounds for haddock, along with other fish species such as Atlantic cod (*Gadus morhua*) and herring (*Clupea harengus*) (Olsen et al., 2010). Proposals for petroleum extraction in these areas are controversial because of the deleterious impact this activity could have on spawning fish (Misund and Olsen, 2013), and we recently showed that haddock embryos are especially vulnerable to toxic effects of dispersed crude oil (Sorhus et al., 2015).

Oil spills in critical areas for fish spawning or aquaculture have proven to be a recurrent worldwide problem. Generally the embryos of marine fish are sensitive to developmental toxicity of crude oil, which causes embryonic heart failure by disrupting cardiac function and morphogenesis through inhibition of excitation–contraction (E–C) coupling (Brette et al., 2014; Incardona et al., 2014, 2015, 2005). Severe heart defects in embryos are also associated with craniofacial malformations. Deformation of the craniofacial skeleton can be secondary to oedema or loss of circulation (Incardona et al., 2004); however, the specific craniofacial phenotype of haddock embryos exposed to crude oil suggests a direct effect (Fig. S1). It remains to be determined whether craniofacial malformations observed in haddock embryos arise from the disruption of independent or common regulatory pathways involved in development of the heart and craniofacial skeleton.

Irrespective of the sensitivity of haddock to crude oil toxicity, as a non-model organism this species provides a number of pertinent features that make it an ideal subject for developmental studies. There are established captive broodstock methods (Moksness et al., 2004), and haddock are broadcast spawners that produce large numbers of embryos providing sufficient mass for biochemical or analytical chemical analyses. The embryos are large and spectacularly translucent, with less pigment than zebrafish, for example. For a temperate species, the developmental rate provides a balance between fast enough for several experiments within a spawning season and slow enough for detailed, quantitative live microscopy. Atlantic haddock thus makes an excellent bridge between zebrafish and other non-model fish with less readily available embryos.

Here we deeply sampled the transcriptome of Atlantic haddock throughout distinct stages of the embryonic to early larval period, linking mRNA levels to microscopically visible structures. The assembly and annotation was based on the previously characterised genome of a closely related gadiform, Atlantic cod (Star et al., 2011). In addition to a more complete description of all differentially expressed genes (DEGs) and connecting global patterns to phenotypic staging, we specifically focused on signalling pathways and structural genes involved in the developing cardiovascular system and craniofacial skeleton, since these structures are especially affected by crude oil exposure. Standard bioinformatics approaches were used to characterize cellular and developmental pathways. However, bioinformatics software applications typically rely on databases derived from published literature establishing gene interaction networks in model systems, and are also heavily biased towards mammalian species. In order to compare gene expression levels in haddock to expected tissue-specific patterns, for all focal genes we performed individual searches in the Zfin.org gene expression database for patterns established by in situ hybridization. In cases where zebrafish data were lacking, we relied on published patterns in chick or mouse embryos. We anticipate that these data will provide the basis for identifying mechanisms underlying abnormal development in a broader array of fish species, which in turn will augment the development of quantitative tools to assess the impacts of oil spills and other environmental changes on fish spawning grounds worldwide.

2. Results and discussion

2.1. General transcriptome dynamics

Developmental staging of haddock embryos and larvae was based on a previous description (Fridgeirsson, 1978), with some modifications based on more recent work (Martell et al., 2005) and our own observations. We sequenced RNA from eight stages, including blastula (*Blastula*, 12 day° (dd)); moment of optic bulbs formation (*Optic bulb*, 24 dd); end of organogenesis 1 or formation of preorgans (*Organ 1*, 36 dd); first heartbeat (*Heartbeat*, 48 dd); end of organogenesis 2 or full development of main organs (*Organ 2*, 78 dd); preparation for hatch to 50% hatch (*Hatching*, 102 dd); yolk sac larva with functional eyes (*Ys larva*, 126 dd); and first feeding larva (*Ff larva*, 158 dd). The number of up- and down-regulated DEGs in each transition, respectively, were 8275 and 3523 in blastula to moment of optic bulbs (12–24 dd), 4329 and 1341 in moment of optic bulbs to end of organogenesis 1 (24–36 dd), 3033 and 1035 in end of organogenesis 1 to first heart beat (36–48 dd), 5390 and 4863 in first heart beat to end of organogenesis 2 (48–78 dd), 5710 and 4622 in end of organogenesis 2 to hatching stage (78–102 dd), 2907 and 4751 in hatching stage to yolk sac larva (102–126 dd) and 2623 and 3568 in yolk sac larva to first feeding larva (126–158 dd) (Fig. 1A). The corresponding numbers for DEGs with a fold change (FC) of 10 or more for up- and down-regulated genes were 2200 and 407 (total 2607), 480 and 14 (total 494), 159 and 11 (total 170), 565 and 22 (total 587), 294 and 6 (total 300), 51 and 5 (total 56) and 10 and 9 (total 19) genes, respectively (Fig. 1B). The largest difference was between blastula and moment of optic bulbs (12–24 dd), both when referring to number of DEGs in total and in genes regulated 10-fold or more. The large changes in gene expression associated with this transition are consistent with both decay of maternal transcripts (seen as down-regulation) and early phases of zygotic transcription. The complete list of genes with normalised expression values for all stages of development, with NOISeqBIO probability and FC for all genes and transitions, can be found in the Supplementary dataset 1.

2.2. KEGG pathways

We linked DEGs to KEGG pathways in order to identify their systems-level function. “Housekeeping” genes can dominate among DEGs in transcriptomic studies due to their large number of constituent genes, while smaller more specialised pathways may be masked. To increase the probability of identifying more specialised developmental pathways containing genes that are predominantly up-regulated, we calculated the ratio between the number of up- and down-regulated genes within each specific pathway using the equation (up-regulated+1)/(down-regulated+1; Fig. 2A). The “+1” transformation of the data is conducted to avoid dividing by zero in pathways without down-regulated DEGs.

Because the heart is a major target organ for crude oil toxicity, we focused on genes and pathways involved in cardiac development and function. KEGG pathway “Cardiac muscle contraction” was represented among the 10 most up-regulated pathways from all transitions, except between blastula and formation of optic bulbs, and hatching and yolk sac larva (Fig. 2A). The cardiac contraction KEGG pathway includes many genes that function in E–C coupling. Many of these genes were up-regulated in the transition between moment of optic bulbs and end of organogenesis 1 (Fig. 2B). Most genes in this pathway continued to show a pattern of up-regulation until the transition from hatching to yolk sac larva, where expression is mostly unchanged.

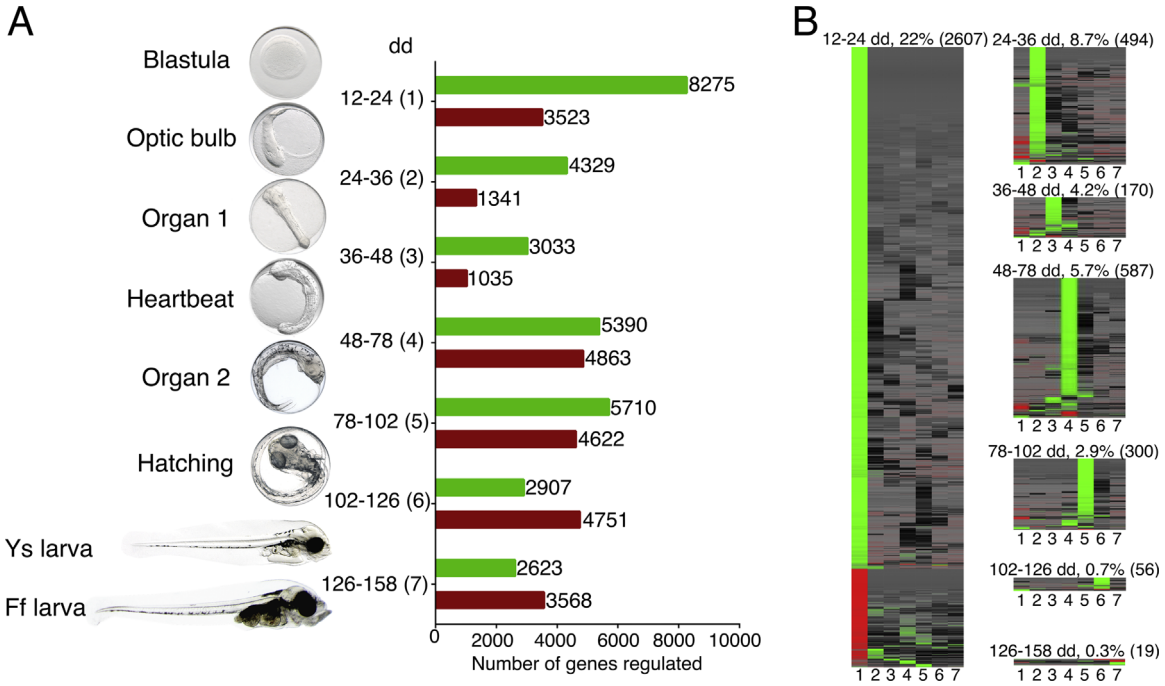

Fig. 1. Overview over stages and Differentially Expressed Genes (DEGs) (A) number of DEGs in each of the 7 transitions between the 8 stages of development, from 12 dd to 158 dd. Stage identification and representative image are indicated on the left, degree-days of stages in the centre, with bars representing numbers of up-regulated (green) and down-regulated (red) DEGs for each transition. Blastula (*Blastula*,12 dd); Moment of optic bulbs (*Optic bulb*, 24 dd). End of organogenesis 1 (*Organ 1*, 36 dd); First heart beat (*Heartbeat*, 48 dd); End of organogenesis 2 (Organ 2, *78 dd*); Preparation for hatch, 50% hatch (*Hatching*, 102 dd); Yolk sac larva (*Ys larva*, 126 dd); First feeding larva (*Ff larva*, 158 dd) (B) Heat maps representing DEGs with more than 10 fold difference in each transition. The percentage of fold change (FC) ≥ 10 of total DEGs is given for each transition, and total number of DEGs with FC ≥ 10 in parentheses. Green and red indicate up- or down regulation, respectively, black indicates constant expression between the stages.

2.3. Most up-regulated genes in relation to KEGG pathways

By two-way comparisons between each of the transitions we identified the ten most highly up-regulated genes based on FC, and compared their expression levels across each stage (Fig. 3).

2.3.1. Blastula to moment of optic bulbs, 12–24 dd

The transition from blastula to moment of optic bulbs (Fig. 3A) was dominated by transcription factors and DNA interacting genes, including SIX homeobox 3 (*six3*), paired box 3 (*pax3*), FEZ family zinc finger 2 (*fezf2*), zinc finger and BTB domain containing 16a (*zb16a*), nuclear receptor subfamily group F member 5 (*nr2f5*), sp8 transcription factor b (*sp8b*) and homeobox protein Hox-D4b (*hxd4b*). Up-regulation of these genes is consistent with a role for these major transcription factor families in early embryonic development and formation of specific structures at these stages. For example, expression of *six3* can be linked to the formation of the eyes (Inbal et al., 2007), while *pax3* function is required in early neural tube development (Moore et al., 2013) and somitogenesis (Hammond et al., 2007) in zebrafish, both of which are well underway by the end of this transition (18–20 somites). In addition, two oxidases, aldehyde dehydrogenase family 1 member 3 (*al1a3*) and eosinophil peroxidase (*epx*) and a multifunctional apolipoprotein, beta-2-glycoprotein 1 (*apoh*) were represented. Several of the KEGG pathways with highest up/down-regulated ratios (Fig. 2A) represent pathways involved in transcription and translation (e.g., non-homologous end-joining, mismatch repair, ribosome, aminoacyl tRNA biosynthesis, homologous recombination), emphasising the onset of zygotic transcription just prior to this transition.

2.3.2. Moment of optic bulbs to end of organogenesis 1, 24-36 dd

In the transition from moment of optic bulbs to end of organogenesis 1 (Fig. 3B), the ten most up-regulated genes were those encoding muscle-associated proteins desmin (*des*) and cardiac muscle myosin heavy chain 6 (*myh6*), collagens type I alpha 1 (*co1a1*) and type IX alpha 2 (*co9a2*), a gamma-crystallin m2 (*crgm2*), lipophilin (*plp*), kelch repeat and BTB domain-containing protein 10 (*kbtba*) and immunoglobulin superfamily, DCC subclass, member 3 (*igdc3*). "Cardiac contraction" was the pathway with the highest ratio, consistent with the onset of cardiac development and formation of cardiac muscle cells (Dirkx et al., 2013). Also up-regulation of the collagens *co1a1* and *co9a2* is consistent with their expression in developing somites and notochord, respectively (Thisse et al., 2001).

2.3.3. End of organogenesis 1 to first heart beat, 36-48 dd

From the end of organogenesis 1 to first heartbeat (Fig. 3C), the most up-regulated DEGs were two gamma-crystallins, m2 (*crgm2*) and m3 (*crgm3*), palmdelpin (*palmd*), sodium-coupled monocarboxylate transporter 1 (*sc5a8*) and the muscle associated proteins cardiac troponin T type 2 (*tnnt2*), skeletal muscle myosin heavy chain 1 (*myh1*) and four other paralogues of myosin heavy chain (*myss*). The pathway "cardiac muscle contraction" was still one of the pathways with the highest up-/down-regulated ratio, consistent with the highly expressed myofibrillar structural genes, *tnnt2*, *myh1* and *myss*. These findings are expected based on observation of the first heartbeat around 48 dd.

2.3.4. First heartbeat to end of organogenesis 2, 48-78 dd

In the transition from first heartbeat to end of organogenesis 2 (Fig. 3D) the ten most up-regulated DEGs were those encoding the calcium associated proteins calsequestrin 1 (*casq1*) and calcium binding protein 5 (*cabp5*); arrestin-C/retinal cone arrestin-3 (*arrc*), ADP-ribosylation factor-like protein 3 (*arl3*), gliomedin (*gldn*), aquaporin 8 (*aqp8*); two genes encoding DNA interacting proteins, BTB/POZ domain containing protein 17 (*btbdh*) and leucine-rich repeat containing protein 30 (*lrc30*); and two paralogues of immunoglobulin-like

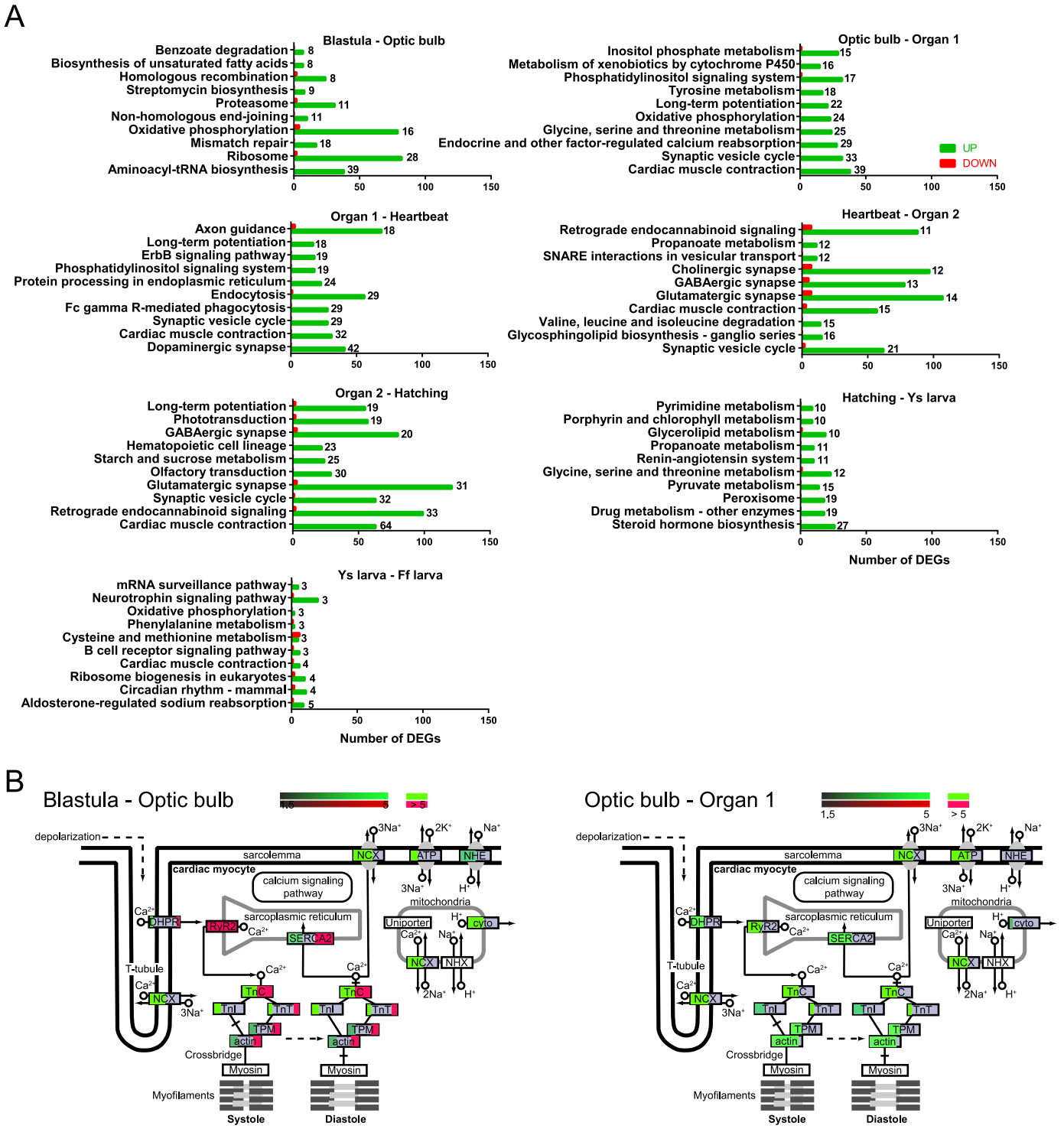

Fig. 2. KEGG pathway analysis. (A) Identification of the 10 most highly up-regulated KEGG pathways using ratios. Bars represent number of DEGs (FC ≥ 1.5) up-regulated (green) and down-regulated (red) for each transition with the ratio indicated beside each bar. (B) Schematic of gene products represented in the Cardiac muscle contraction KEGG pathway (modified from www.kegg.jp, Kanehisa Laboratories). DEGs up- (green) or down-regulated (red) are shown for the blastula to moment of optic bulbs transition (left) and moment of optic bulbs to end of organogenesis 1 (right).

and fibronectin type III domain containing protein 1 (*igfn1*). These genes represent multiple organ systems, including the eye (*arrc*), skeletal muscle (*casq1* (Thisse et al., 2001) and *igfn* (Baker et al., 2010)), the peripheral nervous system (*gldn*) (Feinberg et al., 2010), and blood vessels (*aqp8*) (Sumanas et al., 2005; Thisse et al., 2001). Pathways that were highly up-regulated also were consistent with neural development and synaptic activity, including "synaptic vesicle cycle", "glycosphingolipid biosynthesis-ganglio series", "glutamatergic synapse", "GABAergic synapse", "cholinoergic synapse". Relative to the previous transitions, this transition was represented by a larger diversity of organ-specific genes and pathways, consistent with terminal differentiation and late stages of organogenesis.

2.3.5. *End of organogenesis 2 to preparation for hatch, 78-102 dd*

The group of highest up-regulated DEGs in the transition from end of organogenesis 2 to hatching stage (Fig. 3E) was dominated

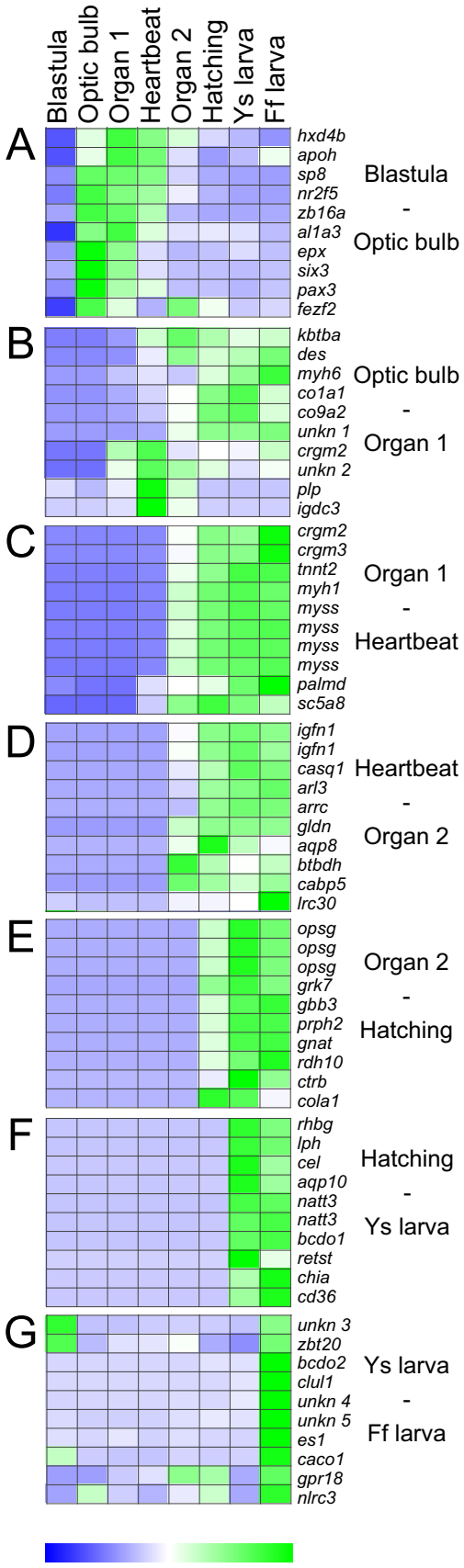

by genes involved in phototransduction, including three green sensitive opsin paralogues (*opsg*), G-protein coupled receptor kinase 7 (*grk7*), guanine nucleotide binding protein beta polypeptide 3 (*gnb3*), peripherin 2 (*prph2*), guanine nucleotide-binding protein G(t) subunit alpha (*gnat*). Other genes were retinol dehydrogenase 10 (*rdh10*) (also potentially involved in retinal function), chymotrypsin B (*ctrb*) and collagen type XXI alpha 1 (*col21a1*). Consistent with these individual genes and the robust pigmentation of the eye observed at this stage (Fig. 1), the most up-regulated pathway was "phototransduction". In addition other highly up-regulated pathways were linked to terminal differentiation and function of the nervous system, such as "olfactory transduction" together with others related to synaptic function (Fig. 2A).

2.3.6. *Preparation for hatch to yolk sac larva, 102-126 dd*

From hatching stage to yolk sac larva (Fig. 3F), several of the ten most highly up-regulated genes were involved in the digestive system, including lactase-phlorizin hydrolase (*lct*), carboxyl ester lipase (*cel*), aquaporin-10 (*aqp10*) (Mobasheri et al., 2004), beta-carotene 15,15 monooxygenase (*bmco1*), and acidic mammalian chitinase (*chia*). Other highly expressed genes included platelet glycoprotein 4 (*cd36*), two paralogues of natterin-3 (*natt3*), Rh family B glycoprotein (*rhgb*), and putative all-trans-retinol 13,14 reductase (*retsat*). Most pathways among the top ten were involved in metabolic processes. These highly represented genes and pathways are consistent with preparation for exogenous feeding.

2.3.7. *Yolk sac larva to first feeding larva, 126-158 dd*

The transition from yolk sac larva to first feeding larva showed markedly fewer highly up-regulated genes than the other transitions (Fig. 1B). The top ten most up-regulated DEGs (Fig. 3G) were Zinc finger and BTB domain containing 20 protein (*zbtb20*), beta-carotene 9,10-oxygenase (*bco2*), clusterin-like protein 1 (*clu1*), calcium-binding and coiled-coil domain containing protein 1 (*calcoco1*), ES1 protein, mitochondrial (*es1*), NLR family CARD domain containing 3 (*nlrc3*) and N-arachidonyl glycine receptor (*gpr18*). These genes are scattered across diverse processes, and specific pathways were sparsely represented. This finding is consistent with the absence of major structural changes between these stages. However, one pathway that stood out was "B-cell receptor signalling pathway". While development of immune cells is not a simple visible phenotype, B-cell development was recently shown to be initiated in first feeding stage zebrafish larvae (Danilova and Steiner, 2002).

2.4. *Development of the cardiovascular system and craniofacial skeleton*

Pathways orchestrating the development of the heart and craniofacial skeleton contain a large number of genes, some common to both and also used in the formation of other organs. We thus selected a subset of genes known to play prominent roles or suspected to be associated with abnormal phenotypes arising from crude oil exposure and other environmental impacts.

2.4.1. *Cardiovascular system*

Specific genes involved in the development or function of the cardiac system (Staudt and Stainier, 2012) have been divided into four categories: (I) Cardiogenesis, (II) Vasculogenesis and

Fig. 3. Most up-regulated genes. The 10 most up-regulated genes in each transition based on fold change. (A) Blastula to moment of optic bulb, (B) moment of optic bulb to end of organogenesis 1, (C) end of organogenesis 1 to first heart beat, (D) first heart beat to end of organogenesis 2, (E) end of organogenesis 2 to preparation for hatch, (F) preparation for hatch to yolk sac larva and (G) yolk sac larva to first feeding larva. Heat maps show normalised normalised total read count in every stage for the indicated genes, described by their Swiss-Prot gene symbol.

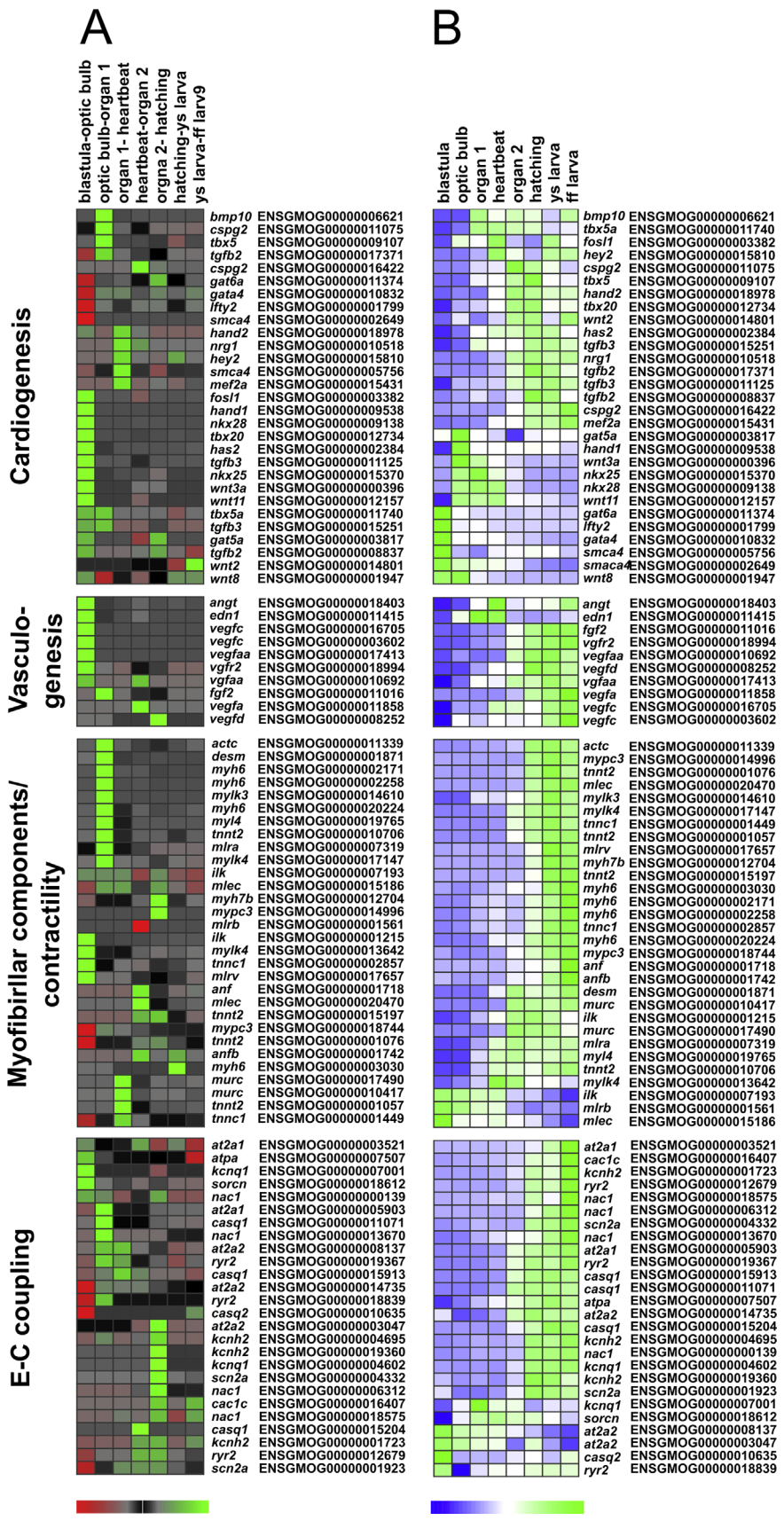

Fig. 4. Expression of genes involved in cardiovascular system development. Heatmaps represent (A) normalised fold change in all transitions with up-regulation in green, down-regulation in red and no change in expression in black; and (B) normalised total read count in all stages, with low relative expression in blue and high relative expression in green. Paralogues with no change in expression over the examined period were excluded.

angiogenesis, (III) Myofibrillar components/contraction, (IV) Excitation–Contraction (E–C) coupling (Fig. 4; A, fold change between transitions; B, normalised total read count).

Cardiogenesis involves a number of complex transcriptional networks and signalling pathways (Bruneau, 2002; Dirkx et al., 2013; Lyons, 1996; Smith et al., 2008; Stainier et al., 1993; Zhou et al., 2011). Key genes selected within this category included several involved in determination of cardiac progenitor cells and differentiation of cardiomyocytes, such as the transcriptional regulators *fosl1, hand1, nkx28, tbx20, mef2a, nkx25, gata4, gat5a, gat6a, tbx5, tbx5a, hey2, hand2,* and *smca4,* and signalling molecules and their modifiers *bmp10, lfty2 wnt2, wnt3a, wnt8, wnt11, nrg1, tgfb2, tgfb3, cspg2,* and *has2.* A larger number of genes were up-regulated in the transition from blastula to moment of optic bulbs (Fig. 4A), including *fosl1, hand1, nkx28, tbx20, has2, tgfb3, nkx25, tgfb3, tgfb2* (ENSGMOG00000008837)*, gat5a, tbx5a, mef2a, wnt3a and wnt11.* A smaller number of genes were highly up-regulated at the subsequent transitions (Fig. 4A), with three for moment of optic bulbs to end of organogenesis 1 (*bmp10, tbx5 and tgfb2* (ENSGMOG00000017371)), and four for end of organogenesis 1 to first heartbeat (*hand2, nrg1, hey2* and *smca4* (ENSGMOG00000005756)). Three patterns in transcript expression were observed: those mainly expressed at the blastula stage, those expressed most highly from moment of optic bulbs to first heartbeat, and those highly expressed from end of organogenesis 1 onward (Fig. 4B). Only five genes, *gat6a, lfty2, gata4*, *smca4 (*ENSGMOG00000002649) and *wnt8,* were highly expressed at blastula stage (Fig. 4B) and all except for *wnt8* were therefore mainly down-regulated in the blastula to moment of optic bulbs transition (Fig. 4A). Several of the selected transcription factors function in early determination of cardiac precursors (Lyons, 1996; Staudt and Stainier, 2012), and the results with *gat6a*, *lfty2, gata4* and *smca4* (ENSGMOG00000002649) are consistent both with such a role and the timing of early heart development in haddock. Transcriptional regulators of cardiogenesis like *nkx25, nkx28, gata4, gat5a, gat6a, fosl1* and *smca4* were most highly expressed in the earliest stages before first heartbeat.

Vasculogenesis gives rise to new blood vessels, while angiogenesis is responsible for the remodelling and expansion of this network (Fish and Wythe, 2015). In addition, the development of the endocardium utilises some of the same signalling pathways as vasculogenesis and angiogenesis. The genes included in the category were *edn1, angt, vgfr2, vegfd* and two paralogues each of *vgfaa, vegfc* and *vegfa*. All of these genes showed highest expression in later developmental stages (Fig. 4B). In particular, the vascular endothelial growth factor related genes were strongly up-regulated at the blastula to moment of optic bulbs (Fig. 4A), but reached peak expression at the larval stages. This is consistent with a known role for vegf-related genes in early development of both the heart and vasculature (Dietrich et al., 2014; Patan, 2000), followed by the more dramatic elaboration of blood vessels in late embryonic and early larval stages (Childs et al., 2002; Isogai et al., 2001).

The contractile apparatus consists of myofibrillar structural proteins and other sarcomeric, structural and regulatory components. In addition there are homoeostatic regulators of contractility. The myofibrillar components/contractility category includes genes encoding troponins (*tnnc1* and *tnnt2*), myosin related proteins (*myh6, myh7, myh7b, myl4, mlra, mlek, mlrb, mlrv, mylk4, mylk3, mypc3, murc*), actin (*actc*), integrin-linked protein kinase (*ilk)*, desmin (*des*) and the natriuretic peptides (*anf, anfb*). All of these genes were most highly expressed at later stages of development (Fig. 4B), except for *mlrb* and *ilk* (ENSGMOG00000007193), suggesting that these genes have functions in early organogenesis. Most myosin-related genes were up-regulated in the transition from moment of optic bulbs to first heartbeat (Fig. 4A). In contrast the troponins (four troponin T2 and two troponin C paralogues) showed a more complicated pattern of regulation, with different paralogues up-regulated at different stages, including some very early, before cardiogenesis. The myosin expression pattern is consistent with myofibril assembly prior to the first heartbeat (Fridgeirsson, 1978). While we do not know the identity of the haddock troponin T paralogues at this point, zebrafish paralogues have differential tissue specificity and are not necessarily restricted to cardiomyocytes (Thisse et al., 2001). The pattern observed here suggests that at least one of the paralogues that is up-regulated later in organogenesis is the cardiac-specific isoform.

E–C coupling links electrical excitation to myofiber contraction in cardiomyocytes through a cycle of depolarisation–repolarisation (Alday et al., 2014; Garcia et al., 2012; Liang et al., 2014; Rosati and McKinnon, 2004; Sanguinetti and Tristani-Firouzi, 2006). E–C coupling in fish cardiomyocytes involves voltage-gated Na^+, Ca^{2+}, and K^+ channels, as well as other Ca^{2+}-regulated channels and Ca^{2+}-binding proteins. Included in this category were genes encoding ion channels (*at2a1, at2a2, cac1c, kcnh2, kcnq1, nac1, scn2a*), ryanodine receptor 2 (*ryr2*), ATP synthase (*atpa*), and calcium handling proteins calsequestrin (*casq1, casq2*) and sorcin (*sorcn*). As observed for myofibrillar genes, E–C coupling genes showed two patterns, one consistent with up-regulation during cardiac development or a more complicated pattern with earlier up-regulation (Fig. 4). For example, the latter pattern was observed for paralogues of both ryanodine receptor, sarcoplasmic reticulum calcium pump families and one voltage gated sodium channel paralogue (*ryr2*, *at2a1* and *at2a2*, and *scn2a* (ENSGMOG00000004332), respectively). These genes are known to be expressed in a variety of tissues, some very early in zebrafish development (Thisse et al., 2001). While there are roles for calcium signalling in early teleost development, these roles are not well characterised at the level of specific channels involved (Webb et al., 2011). The high expression of *ryr2* (ENSGMOG00000018839), and the two *at2a2* paralogues (ENSGMOG00000008137 and ENSGMOG00000003047) at the blastula stage and their dynamic regulation at the blastula to optic bulbs transition suggest a potentially novel role for these genes in early development. In contrast, other genes encoding E–C coupling proteins in cardiomyocytes (*cac1c, nac1, kcnh2, kcnq1, at2a2* (ENSGMOG00000003047), *scn2a* (ENSGMOG00000004332) and *ryr2* (ENSGMOG00000012679)), were highly up-regulated after the first heartbeat as expected (Alday et al., 2014; Arnaout et al., 2007; Garcia et al., 2012; Ramachandran et al., 2013; Rosati and McKinnon, 2004).

2.4.2. Craniofacial and skeletal development

Although the skeleton comprises fairly simple organs with few cell types, craniofacial organogenesis involves the complex orchestration of multiple inductive signalling pathways combined with the intricate movements of neural crest cells (NCCs) (Minoux and Rijli, 2010; Szabo-Rogers et al., 2010). Like other vertebrates, the bones of the fish head can be roughly divided into two groups, those of the neurocranium (skull) and the pharyngeal bones that make up the jaw and gill support structures (Kimmel et al., 2001). We based our selection of genes both on the processes underlying this broad division of bone structures and on phenotypes related to crude oil toxicity (Lefebvre and Bhattaram, 2010). We divided genes involved in craniofacial and skeletal development into three categories: (I) Neural crest cell (NCC) migration and identity; (II) Craniofacial morphogenesis and growth (Craniofacial), including genes involved in palatogenesis and planar cell polarity; and (III) Bone and cartilage structure and mineralisation (Structural) (Fig. 5; A, fold change between transitions; B, normalised total read count).

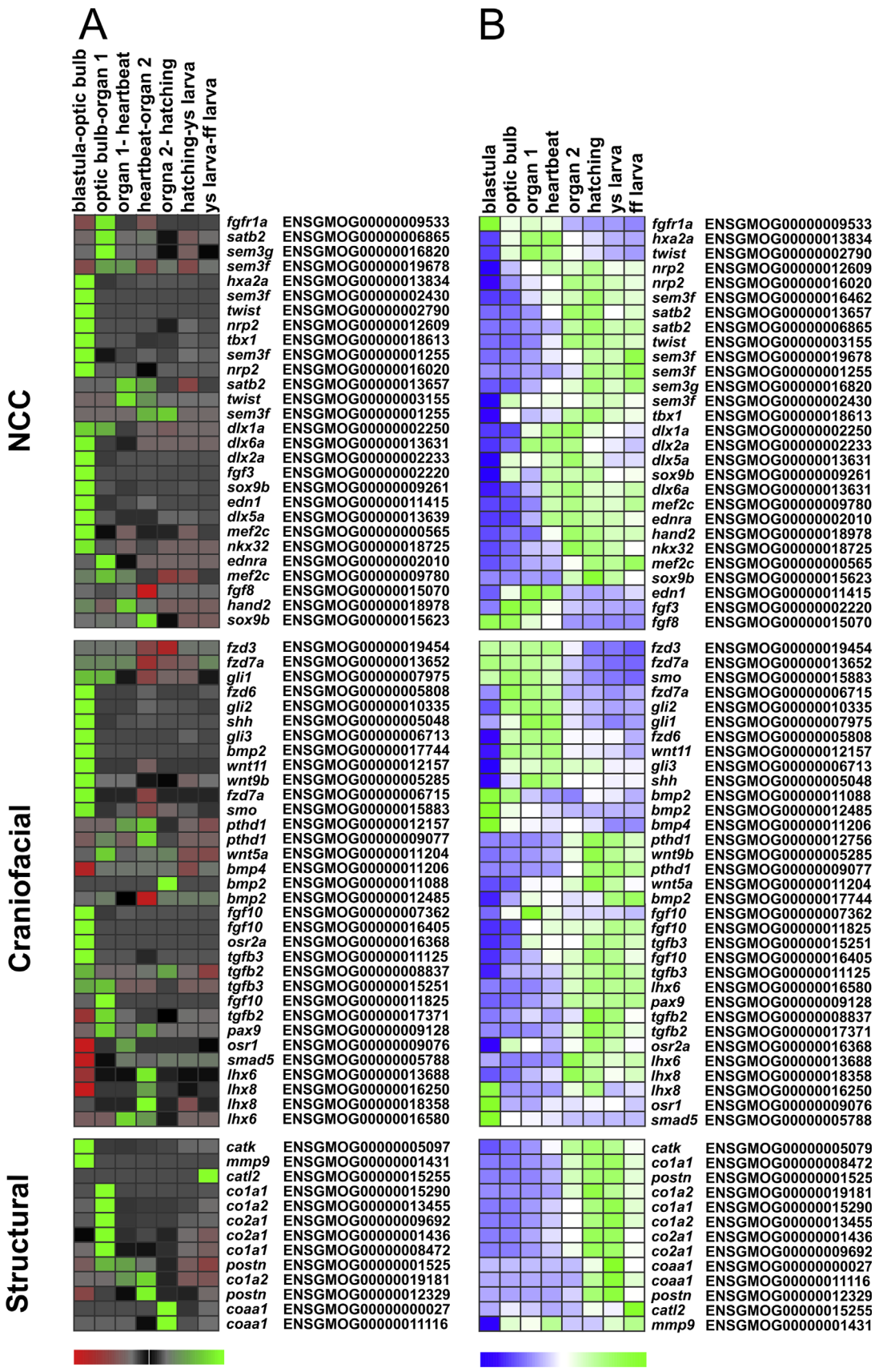

Fig. 5. Expression of genes involved in craniofacial and skeletal development. Heatmaps represent (A) normalised fold change in all transitions with up-regulation in green, down-regulation in red and no change in expression in black; and (B) normalised total read count in all stages, with low relative expression in blue and high relative expression in green. Paralogues with no change in expression over the examined period were excluded.

NCCs are a migratory cell population specific to vertebrates. NCC induction, migration and positional identity are choreographed by complex molecular mechanisms (Minoux and Rijli, 2010; Simoes-Costa and Bronner, 2015). NCC migratory streams are sculpted in part by the expression of *nrp2a* and *nrp2b* receptors in migrating NCCs, their repulsive ligands *sem3f* and *sem3g* in adjacent NCC free zones, and *fgfr1a* in tissue surrounding NCCs. Segregation of NCC subpopulations within pharyngeal arches is also guided by *twist* and *tbx1* expression, and genes such as *hxa2, satb2* and *sox9* have a role in pharyngeal arch patterning (Minoux and Rijli, 2010). Of all these genes, only *fgfr1a* had its peak expression at the blastula stage (Fig. 5B). In the transition from blastula to moment of optic bulbs, NCC genes that were up-regulated included the two paralogues of *nrp, sem3f* (ENSGMOG00000016462), *sem3f* (ENSGMOG00000002430), *tbx1*, *twist* (ENSGMOG00000002790), *hxa2* and *sox9b* (ENSGMOG00000009261) (Fig. 5A). In the transition from moment of optic bulbs to end of organogenesis 1, *Sem3g* together with *sem3f* (ENSGMOG00000019678), *satb2* (ENSGMOG00000006865) and *fgfr1a* were up-regulated, *twist1* (ENSGMOG00000003155) and *satb2* (ENSGMOG00000013657) were up-regulated in the two subsequent transitions, while the *sem3f* (ENSGMOG00000001255) paralogue was up-regulated in the transition from first heartbeat to end of organogenesis 2. The early up-regulation of most genes is consistent with their roles in early NCC patterning events, while some paralogues (e.g., ENSGMOG00000001255) may have other functions. Notably, many of these genes involved in early NCC development reach their peak expression levels at stages after organogenesis is complete (Fig. 5B).

NCC positional identity is established by the signalling molecule *edn1* and its receptor *ednra*, *dlx5* and *6* (transcription factors downstream of EDN1), *hand2, nkx32* and two paralogues of *mef2c*, where MEF2C is thought to act as a direct transcription activator for *dlx5/6* (Minoux and Rijli, 2010; Szabo-Rogers et al., 2010). In the transition from blastula to moment of optic bulbs, *edn1, dlx5a*, *dlx6*, *nkx32* and *mef2c* (ENSGMOG00000000565) were up-regulated, while *ednra* and *mef2c* (ENSGMOG00000009780) were up-regulated in the following transition, moment of optic bulbs to end of organogenesis 1. Although *hand2* was up-regulated in the blastula to moment of optic bulbs transition, it was more strongly up-regulated from the end of organogenesis 1 to first heartbeat (Fig. 5B). Products of *fgf8* and *fgf3* act as both key NCC survival factors and chemoattractants to promote the correct patterning of NCC-derived skeletal elements (Minoux and Rijli, 2010). Here *fgf8* was expressed most highly in early stages including blastula, and consequently down-regulated in the first heartbeat to end of organogenesis 2 transition (Fig. 5). The *fgf3* gene was mainly expressed in the early stages, except blastula, and was consequently up-regulated in the blastula to moment of optic bulbs transition. Notably, genes encoding the signalling molecules (*edn1*, *fgf3*, *fgf8*) reached their peak expression levels prior to their downstream effectors (e.g., the *dlx* genes) (Fig. 5B).

Other signalling pathways included in the Craniofacial category are the hedgehog, BMP, and non-canonical Wnt pathways, which also include ligands, receptors and downstream effectors (Szabo-Rogers et al., 2010). Sonic hedgehog (Shh) is important for midline signalling in craniofacial development, and in particular for development of the anterior neurocranium (or palate) in fish (Wada et al., 2005), while BMP molecules are involved in jaw patterning, as well as other roles (Minoux and Rijli, 2010). Both canonical and non-canonical Wnt signalling pathways are involved in proper outgrowth of craniofacial skeletal elements (Szabo-Rogers et al., 2010). Hedgehog signalling genes included *shh*, the receptors Patched 1 (*pthd1*) and Smoothened (*smo*) and the transcription factors *gli1, gli2* and *gli3* (Nozawa et al., 2013; Szabo-Rogers et al., 2010). Genes representing the non-canonical Wnt signalling in the craniofacial category were *wnt5a, wnt11, fzd3, fzd6* and *fzd7a*. Finally, we identified genes for BMP2 and BMP4. Two *bmp2* paralogues (ENSGMOG00000011088 and ENSGMOG00000012485), and *bmp4* were highly expressed in the blastula stage (Fig. 5B), and the latter gene was down-regulated in the transition from blastula to moment of optic bulbs (Fig. 5A). Genes that were up-regulated in this transition included *shh, smo*, *gli1*, *gli2* and *gli3,* and *wnt9b, wnt11*, *fzd6* and *fzd7a* (ENSGMOG00000006715) (Fig. 5A). *Gli1* was up-regulated to an even higher level in the subsequent transition (moment of optic bulbs to end of organogenesis 1). The other *fzd7a* paralogue (ENSGMOG00000013652) was highly expressed in the four first stages, and down-regulated in the first heartbeat to end organogenesis 2. The single *fzd3* gene showed a similar pattern. In the transition from moment of optic bulbs to end of organogenesis 1, *wnt5a* was up-regulated and expressed most highly at the latest stages examined. Almost all of these genes were up-regulated relatively early and reached their peak expression prior to the end of organogenesis, consistent with their known roles in pattern formation.

The gross jaw malformation (facial shortening) observed in oil-exposed haddock is suggestive of abnormal palatogenesis or growth of the ethmoid plate (DeLaurier et al., 2012; Sorhus et al., 2015). Therefore we specifically focused on haddock genes known to be necessary for palatogenesis from studies in zebrafish (Swartz et al., 2011). Included here were the transcription factors *osr1, osr2a, pax9,* and two paralogues of *lhx6* and *lhx8,* signalling molecules *tgfb2* and *tgfb3* (two paralogues each), *smad5* and three paralogues of *fgf10*. This category also includes members of the hedgehog and BMP pathways already described above. Only, *smad5*, *osr1* and *lhx8* (ENSGMOG00000016250) were highly expressed in the blastula stage (Fig. 5B). Therefore, *smad5*, *osr1* and *lhx8* (ENSGMOG00000016250) were down-regulated in the first transition (Fig. 5A). The rest had higher expression in later stages (Fig. 5B), except for *fgf10* (ENSGMOG00000007362), which was most highly expressed in the end of organogenesis 1 and first heartbeat stage. A group of genes (*osr2a*, *fgf10* (ENSGMOG00000007362 and ENSGMOG00000016405), *tgfb2* (ENSGMOG00000017371) and *tgfb3* (ENSGMOG00000015251 and ENSGMOG00000011125)) were up-regulated in the first transition, while several had a more dynamic regulation throughout development (*tgfb2* (ENSGMOG00000008837 and ENSGMOG00000017371), *tgfb3* (ENSGMOG00000015251), *fgf10* (ENSGMOG00000011825), *pax9*, both *lhx6* paralogues and *lhx8* (ENSGMOG00000018358)) (Fig. 5A). In the absence of information regarding tissue localisation, it is likely that the gene paralogues specifically functioning in palatogenesis may be those that peak at later stages. Given the involvement of many of these genes in other processes, it is not surprising that their peak expression is not tightly linked to the timing of palatogenesis.

The final category includes genes encoding structural proteins of cartilage and bone matrices. Several collagens are represented (*co1a1, co1a2, co2a1, coaa*) in addition to other proteins secreted by osteoclasts and osteoblasts (*mmp9, catk, postn*) (Berendsen and Olsen, 2015; Merle et al., 2014; Okada et al., 1995; Olsen et al., 2000; Troen, 2004). Collagens are abundant structural components of the extracellular matrix in connective tissue, but also have critical roles in skeletal development (Berendsen and Olsen, 2015; Olsen et al., 2000). Proteases such as matrix metalloproteinase 9 (MMP9) and cathepsin K (CATK) mediate the bone resorbing action of osteoclasts (Okada et al., 1995; Troen, 2004). Although both are important for differentiation of osteoclasts and ossification (Delaisse et al., 2003), their earlier expression here most likely reflects broader functions throughout development. Osteocalcin is a commonly used biomarker for bone development and ossification (Lee et al., 2000), but was not expressed in the period examined here. Finally, periostin (*postn*), a secreted extracellular

protein, is thought to regulate osteoblast cell adhesion, an event that is a requisite for differentiation of osteoblasts (Horiuchi et al., 1999; Litvin et al., 2004).

The collagens were expressed in later stages, and most seem to be up-regulated in the transition from moment of optic bulbs to end of organogenesis 1, except for *co1a2* and *coaa1*, which were most up-regulated in the transitions from first heartbeat to end of organogenesis 2, and end of organogenesis 2 to hatching, respectively (Fig. 5A). Both *mmp9* and *catk* genes were up-regulated in the blastula to moment of optic bulbs transition (Fig. 5) and were continuously expressed throughout development. Two paralogues of *postn* were present. One (ENSGMOG00000012329) was up-regulated in the heartbeat to end of organogenesis 2 transition, while the other (ENSGMOG00000001525) was up-regulated from moment of optic bulbs to end of organogenesis 1, with further up-regulation in the subsequent transition (Fig. 5A). The *postn* paralogues most likely represent *postna* and *postnb* genes, respectively, based on the expression patterns in zebrafish (Thisse et al., 2001). The peak expression of most of these genes in the early larval stage is consistent with complete formation of the initial cartilaginous skeleton.

3. Conclusions

In this study our goal was to link transcriptional changes to developmental processes, specifically pattern formation and organogenesis, in a non-model vertebrate. At each developmental stage examined here in haddock, the most highly expressed genes and pathways were clearly associated with processes occurring at those stages. Importantly, we were able to link gene expression to either the appearance of visible structures (e.g., somitogenesis) or cellular processes characterised in model organisms (e.g., B cell development). These findings indicate the potential of developmental transcriptomics for pinpointing processes that are perturbed in malformed embryos, and understanding pathophysiological mechanisms leading to abnormal development. Many birth defects are spontaneous and not necessarily chromosomally linked (council, 2000), and abnormal development in wild animal populations (e.g., fish embryos affected by oil spills) is more likely due to environmental influences on gene expression. Prior to the advances in deep sequencing, these types of problems were difficult to study or often intractable. Our focus on specific organs that are targets of crude oil developmental toxicity, the heart and craniofacial skeleton, also identified major players controlling these processes. Importantly, in this case also, the selected genes generally showed temporal expression patterns coupled to those processes. For example, expression of signalling molecules preceded expression of downstream effectors.

Few studies have detailed the transcriptomes of developing vertebrates using deep sequencing, in particular with a focus on organogenesis, and none in a non-model organism to our knowledge. Two studies have focused on organogenesis in mouse (Mitiku and Baker, 2007) and human (Fang et al., 2010) embryos, a broader developmental transcriptome has been described for zebrafish (Yang et al., 2013), and the suites of orthologous genes expressed during phylotypic stages were compared for the standard model vertebrates (Irie and Kuratani, 2011). Although the stages assessed in each paper do not necessarily correspond precisely, some key differences are noted between fish and mouse. The stage with the largest number of up-regulated genes in mouse was at the onset of somitogenesis, whereas in fish most up-regulation occurred earlier (i.e., prior to 100% epiboly).

In our experience working on non-model species (Edmunds et al., in press; Incardona et al., 2014; Jung et al., 2015; Kleppe et al., 2014; Sorhus et al., 2015) understanding changes in development on a gene-by-gene or pathway-specific basis is challenging, both in terms of modifying techniques developed in model organisms and the amount of labour involved. Although deep-sequencing approaches are not inexpensive, they are fast and easily applied to non-model organisms. However, it has not been established whether obtaining temporal gene expression patterns through such shotgun approaches can provide information that is relevant for understanding tissue-specific patterns of gene expression. In this case, we have shown that bioinformatics analysis of temporal patterns of gene expression in this non-model fish provides information that closely matches predicted tissue-specific gene expression patterns based on published information in model species (especially zebrafish). Therefore, a comparative transcriptomics approach comparing normal and abnormal embryos will likely reveal critical information relating to disruption of pathways leading to abnormal phenotypes. This will dramatically enhance the dissection of development in non-model organisms by rapidly identifying which genes should be targeted for more in-depth analysis by methods such as in situ hybridisation. The manner in which this transcriptome is linked to visible developmental landmarks will facilitate direct comparisons with other species. Therefore, this publically available developmental transcriptome of haddock provides an important resource for the developmental biology of both model and non-model vertebrates. Finally, coupled with the recently sequenced cod genome, our study is important for understanding the life histories of gadiforms, which support some of the largest commercial fisheries throughout the world.

4. Methods

4.1. Animal collection and maintenance

All animal experiments within the study were approved by NARA, the governmental Norwegian Animal Research Authority (⟨http://www.fdu.no/fdu/⟩, reference number 2012/275334-2). A wild broodstock population of 61 maturing individuals was collected February–March 2013 at spawning grounds in the Austevoll area, on the west coast of Norway, and kept in two 7000 L tanks at the Institute of Marine Research (IMR), Austevoll Research station. The average size of the broodstock fish were 52 ± 7 cm and 1522 ± 519 g and from the size the fish were estimated to be 5 years or more, therefore it is likely that all fish have experienced one to two spawning seasons before they were collected for the experiment. The haddock spawns voluntarily in captivity, and fertilised eggs could therefore be collected from the tanks and transferred to indoor 70 L egg incubators (7.0 °C) or to 2 L glass beakers in a 6 °C climate room. Stages from 12 degree-days (dd) (2 days post fertilisation (dpf) at 6.0 °C) until 48 dd (blastula, moment of optic bulb, end of organgenesis 1, first heartbeat (Fridgeirsson, 1978)) were collected from the glass beakers (continuous light regime). The water was changed every day to maintain optimal conditions and reduce possible bacterial growth. At 70 dd 3×4.1 mL eggs from the incubators were transferred into three 50 L circular tanks. The flow through the tanks was 32 L/hr, the water temperature 8.0 °C, and light regime was 12D:12 L. Light for triplicate tanks was provided by the broad spectrum 2×36 W Osram Biolux 965 (Munich, Germany, www.osram.com) dimmable fluorescent light tubes with 30 min. smooth transitions between light and dark. From four days post hatching (dph), natural zooplankton, mainly copepod nauplii of *Acartia longiremis*, was harvested from the marine pond system "Svartatjern" (van der Meeren et al., 2014) and introduced as feed to the larvae. Increasing amount of zooplankton was added to the growing larvae, from 450,000 to 650,000 zooplankton per tank for 4 dph (134 dd) to

7 dph (158 dd) larvae, respectively. The tanks were further supplemented with marine microalgae concentrate (Instant Algae, Nanno 3600, Reed Marinculture Inc., CA, USA) until termination of the experiment (Karlsen et al., 2015). The embryos started to hatch at 94 dd and 50% hatch was observed at 102 dd (=0 days post hatching). Stages from 78 dd to 158 dd stages were collected from the 50 L tanks. All samples were imaged and inspected in microscope to obtain a synchronic selection and avoid abnormal and dead animals. After inspection, all water was removed before flash-frozen in LN_2 and stored at −80 °C. Staging was performed by images post sampling according to Fridgeirsson's descriptions (Fridgeirsson, 1978).

4.2. Total RNA and cDNA preparation

Total RNA was isolated from frozen pools of animals and individual larvae, two (for 48 dd) or three (rest) replicates from each stage, using Trizol reagent (Invitrogen, Carlsbad, California, USA) according to procedures provided by the manufacturer, which included a DNase treatment step using a TURBO DNA-*free* kit (Life Technologies Corporation). Total RNA from single larvae from 158 dd were extracted using RNeasy micro kit (QIAGEN Sample and Assay Technologies) according to procedures provided by the manufacturer, thereafter total RNA from 5 individuals were pooled for further analysis. The amount of RNA was quantified using a Nanodrop spectrophotometer (NanoDrop Technologies, Wilmington, DE, USA), and quality checked using a 2100 Bioanalyzer (Agilent Technologies, Santa Clara, CA). Absorbance ratio A260: A280 ranged from 1.79 to 2.04 and RNA integrity number (RIN) values ranged from 8.3 to 10. cDNA was subsequently generated using SuperScript VILO cDNA Synthesis Kit (Life Technologies Corporation), according to the manufacturer's instructions. The cDNA was normalised to obtain a concentration of 50 ng/μL.

4.3. Extraction of mRNA, RNA sequencing and bioinformatics

cDNA library preparation and sequencing of three biological replicates per stage (two for 48 dd) was performed by the Norwegian Sequencing Centre (NSC, Oslo, Norway) using the Illumina TruSeq RNA Sample Preparation Kit. Using the multiplexing strategy of the TruSeq protocol six paired end libraries were performed per one lane of the Illumina HiSeq 2000. The raw data has been deposited and can be found at The Sequence Read Archive (SRA) at NCBI (Accession ID: PRJNA287744).

High sequence similarity between cod and haddock justified use of the cod gene model as a template; the average sequence similarity between mapped haddock reads and the cod reference was 98.4%. Out of the 20,954 annotated cod gene models there were 18,833 (89.9%) corresponding haddock genes with at least 10 reads in one sample. Further, we chose to use a verified gene model over a reference-free de novo transcriptome approach to avoid noise from fragmentation and redundancy from un-collapsed genes resulting in a high number of false positives. Thus, the RNA sequencing data was mapped to the coding sequences of the cod gene models (Star et al., 2011) using the Burrows-Wheeler aligner (Li and Durbin, 2009). The cod gene models were annotated with various resources, including Swiss-Prot, Uniref90, GeneOntology and KEGG (Kyoto Encyclopaedia of Genes and Genomes). Samtools idxstat (Li et al., 2009) was used to extract number of mapped reads. The reads were normalised by the total number of mapped sequences. NOISeqBIO (Tarazona et al., 2011) was used to obtain DEGs between the developmental stages (threshold of 0.95). Only genes with 10 reads or more in at least one of the samples were included for further analysis. KEGG pathways analysis (Kanehisa et al., 2012) was performed by mapping the KEGG annotated DEGs from NOISeqBIO to KEGG pathways as described in the KEGG Mapper tool. Heat maps were generated using J-Express by normalising mean and variance at a high level followed by Hierarchical clustering (Dysvik and Jonassen, 2001).

The total number of reads was on average 52.9 million. The mapping efficiency was on average 35.72%, giving an average of 18.9 million 100 bp paired end reads for each group. The UTRs and the mitochondrial genes were not included in the reference gene models, i.e. reads with UTR sequence and all the reads from the mitochondrial genes were excluded from the current data.

4.4. Real time qPCR

Five DEGs from the transcriptome were validated by real-time quantitative PCR (qPCR) (Fig. S2). The genes involved in EC coupling and signalling were specifically picked based on their diversifying expression profile during development. In general, all genes showed the same trend in both methods (Fig. S2). Specific primers and probes for qPCR, (reference gene *ef1α*, and *cp1a, gstp1, ahr2, wnt11, kcnh2, nac1, cac1c* and *at2a2*) were designed with either Primer Express software (Applied Biosystems, Carlsbad, California, USA) or Eurofins qPCR probe and primer design software (Eurofins Scientific, Ebersberg, Germany), according to the manufacturer's guidelines. Primer and probe sequences are given in Table S1. TaqMan PCR assays were performed in duplicate, using 384-well optical plates on an ABI Prism Fast 7900HT Sequence Detection System (Applied Biosystems, Carlsbad, CA, USA) with settings as follows: 50 °C for 2 min, 95 °C for 20 s, followed by a 40 cycles of 95 °C for 1 s and 60 °C for 20 s. No template control, no reverse transcriptase enzyme control and genomic DNA control were included. For each 10-μl PCR reaction, 2.5 ng cDNA was mixed with 200 nM fluorogenic probe, 900 nM sense primer, 900 nM antisense primer in 1xTaqMan Fast Advanced Master Mix (Applied Biosystems, Carlsbad, CA, US). Gene expression data for were calculated relative to the start sample (2 dpf) and using the ΔΔΔCt method generating reference residuals from *ef1a* (technical reference) and *at2a2* (biological reference) in the embryonic and larval exposure, as described in detail in Edmunds et al. (2014). Gene expression data was calculated relative to the first time point (2 dpf) using the ΔΔCt method (Bogerd et al., 2001).

Author contributions

ES, RBE, SM, and SJ conceived and designed the experiments; ES and SM performed the experiments; ES, RBE, JPI, and TF analysed the data; TF contributed reagents/materials/analysis tools; ES, RBE, and JPI wrote the paper.

Competing financial interests

The authors declare no competing financial interests.

Acknowledgements

We would like to acknowledge Stig Ove Utskot, Ørjan Karlsen and Terje van der Meeren for breeding and management of the fish and Penny Swanson for review and comments on the manuscript. This work was financed by the VISTA Foundation (Project no. 6161, www.vista.no) and the Institute of Marine Research, Norway (Project no. 14236, www.imr.no). The funders had no role in study design, data collection and analysis, decision to publish, or preparation of the manuscript

Appendix A. Supplementary material

Supplementary data associated with this article can be found in the online version at http://dx.doi.org/10.1016/j.ydbio.2016.02.012.

References

Alday, A., Alonso, H., Gallego, M., Urrutia, J., Letamendia, A., Callol, C., Casis, O., 2014. Ionic channels underlying the ventricular action potential in zebrafish embryo. Pharmacol. Res. 84, 26–31.

Arnaout, R., Ferrer, T., Huisken, J., Spitzer, K., Stainier, D.Y.R., Tristani-Firouzi, M., Chi, N.C., 2007. Zebrafish model for human long QT syndrome. Proc. Natl. Acad. Sci. USA 104, 11316–11321.

Baker, J., Riley, G., Romero, M.R., Haynes, A.R., Hilton, H., Simon, M., Hancock, J., Tateossian, H., Ripoll, V.M., Blanco, G., 2010. Identification of a Z-band associated protein complex involving KY, FLNC and IGFN1. Exp. Cell Res. 316, 1856–1870.

Berendsen, A.D., Olsen, B.R., 2015. Bone development. Bone 80, 14–18.

Bogerd, J., Blomenrohr, M., Andersson, E., van der Putten, H.H., Tensen, C.P., Vischer, H.F., Granneman, J.C.M., Janssen-Dommerholt, C., Goos, H.J., Schulz, R.W., 2001. Discrepancy between molecular structure and ligand selectivity of a testicular follicle-stimulating hormone receptor of the African catfish (*Clarias gariepinus*). Biol. Reprod. 64, 1633–1643.

Brette, F., Machado, B., Cros, C., Incardona, J.P., Scholz, N.L., Block, B.A., 2014. Crude oil impairs cardiac excitation-contraction coupling in fish. Science 343, 772–776.

Bruneau, B.G., 2002. Transcriptional regulation of vertebrate cardiac morphogenesis. Circ. Res. 90, 509–519.

Childs, S., Chen, J.N., Garrity, D.M., Fishman, M.C., 2002. Patterning of angiogenesis in the zebrafish embryo. Development 129, 973–982.

Council, N., 2000. Scientific Frontiers in Developmental Toxicology and Risk Assessment. National Academies Press, Washington DC, p. 354.

Danilova, N., Steiner, L.A., 2002. B cells develop in the zebrafish pancreas. Proc. Natl. Acad. Sci. USA 99, 13711–13716.

Delaisse, J.M., Andersen, T.L., Engsig, M.T., Henriksen, K., Troen, T., Blavier, L., 2003. Matrix metalloproteinases (MMP) and cathepsin K contribute differently to osteoclastic activities. Microsc. Res. Tech. 61, 504–513.

DeLaurier, A., Nakamura, Y., Braasch, I., Khanna, V., Kato, H., Wakitani, S., Postlethwait, J.H., Kimmel, C.B., 2012. Histone deacetylase−4 is required during early cranial neural crest development for generation of the zebrafish palatal skeleton. BMC Dev. Biol., 12.

Dietrich, A.C., Lombardo, V.A., Abdelilah-Seyfried, S., 2014. Blood flow and bmp signaling control endocardial chamber morphogenesis. Dev. Cell 30, 367–377.

Dirkx, E., Martins, P.A.D., De Windt, L.J., 2013. Regulation of fetal gene expression in heart failure. BBA Mol. Basis Dis. 1832, 2414–2424.

Dysvik, B., Jonassen, I., 2001. J-Express: exploring gene expression data using Java. Bioinformatics 17, 369–370.

Edmunds, R.C., McIntyre, J.K., Luckenbach, J.A., Baldwin, D.H., Incardona, J.P., 2014. Toward enhanced MIQE compliance: reference residual normalization of qPCR gene expression data. J. Biomol. Tech. 25, 54–60.

Edmunds, R.C., Gill, J.A., Baldwin, D.H., Linbo, T.L., French, B.L., Brown, T.L., Esbaugh, A.J., Mager, E.M., Stieglitz, J.D., Hoenig, R., Benetti, D.D., Grosell, M., Scholz, N.L., Incardona, J.P., 2016. Corresponding morphological and molecular indicators of crude oil toxicity to the developing hearts of mahi mahi. Sci. Rep. (in press)

Fang, H., Yang, Y., Li, C.L., Fu, S.J., Yang, Z.Q., Jin, G., Wang, K.K., Zhang, J., Jin, Y., 2010. Transcriptome Analysis of Early Organogenesis in Human Embryos. Dev. Cell 19, 174–184.

Feinberg, K., Eshed-Eisenbach, Y., Frechter, S., Amor, V., Salomon, D., Sabanay, H., Dupree, J.L., Grumet, M., Brophy, P.J., Shrager, P., Peles, E., 2010. A glial signal consisting of gliomedin and NrCAM clusters axonal Na+ channels during the formation of nodes of Ranvier. Neuron 65, 490–502.

Fish, J.E., Wythe, J.D., 2015. The molecular regulation of arteriovenous specification and maintenance. Dev. Dyn. 244, 391–409.

Fridgeirsson, E., 1978. Embryonic development of five species of gadoid fishes in Icelandic waters. Rit Fiskeideildar 5, 1–68.

Garcia, T.I., Shen, Y.J., Crawford, D., Oleksiak, M.F., Whitehead, A., Walter, R.B., 2012. RNA-Seq reveals complex genetic response to deepwater horizon oil release in Fundulus grandis. BMC Genom. 13.

Hammond, C.L., Hinits, Y., Osborn, D.P.S., Minchin, J.E.N., Tettamanti, G., Hughes, S. M., 2007. Signals and myogenic regulatory factors restrict pax3 and pax7 expression to dermomyotome-like tissue in zebrafish. Dev. Biol. 302, 504–521.

Horiuchi, K., Amizuka, N., Takeshita, S., Takamatsu, H., Katsuura, M., Ozawa, H., Toyama, Y., Bonewald, L.F., Kudo, A., 1999. Identification and characterization of a novel protein, periostin, with restricted expression to periosteum and periodontal ligament and increased expression by transforming growth factor beta. J. Bone Miner. Res. 14, 1239–1249.

Inbal, A., Kim, S.H., Shin, J., Solnica-Krezel, L., 2007. Six3 represses nodal activity to establish early brain asymmetry in zebrafish. Neuron 55, 407–415.

Incardona, J.P., Collier, T.K., Scholz, N.L., 2004. Defects in cardiac function precede morphological abnormalities in fish embryos exposed to polycyclic aromatic hydrocarbons. Toxicol. Appl. Pharmacol. 196, 191–205.

Incardona, J.P., Carls, M.G., Teraoka, H., Sloan, C.A., Collier, T.K., Scholz, N.L., 2005. Aryl hydrocarbon receptor-independent toxicity of weathered crude oil during fish development. Environ. Health Perspect. 113, 1755–1762.

Incardona, J.P., Carls, M.G., Holland, L., Linbo, T.L., Baldwin, D.H., Myers, M.S., Peck, K. A., Tagal, M., Rice, S.D., Scholz, N.L., 2015. Very low embryonic crude oil exposures cause lasting cardiac defects in salmon and herring. Sci. Rep. 5, 13499.

Incardona, J.P., Gardner, L.D., Linbo, T.L., Brown, T.L., Esbaugh, A.J., Mager, E.M., Stieglitz, J.D., French, B.L., Labenia, J.S., Laetz, C.A., Tagal, M., Sloan, C.A., Elizur, A., Benetti, D.D., Grosell, M., Block, B.A., Scholz, N.L., 2014. Deepwater Horizon crude oil impacts the developing hearts of large predatory pelagic fish. Proc. Natl. Acad. Sci. USA 111, E1510–E1518.

Irie, N., Kuratani, S., 2011. Comparative transcriptome analysis reveals vertebrate phylotypic period during organogenesis. Nat. Commun. 2.

Isogai, S., Horiguchi, M., Weinstein, B.M., 2001. The vascular anatomy of the developing zebrafish: an atlas of embryonic and early larval development. Dev. Biol. 230, 278–301.

Jung, J.H., Kim, M., Yim, U.H., Ha, S.Y., Shim, W.J., Chae, Y.S., Kim, H., Incardona, J.P., Linbo, T., Kwon, J.H., 2015. Differential toxicokinetics determines the sensitivity of two marine embryonic fish exposed to Iranian Heavy Crude Oil. Environ. Sci. Technol. 49, 13639–13648.

Kanehisa, M., Goto, S., Sato, Y., Furumichi, M., Tanabe, M., 2012. KEGG for integration and interpretation of large-scale molecular data sets. Nucleic Acids Res. 40, D109–D114.

Karlsen, O., van der Meeren, T., Ronnestad, I., Mangor-Jensen, A., Galloway, T.F., Kjorsvik, E., Hamre, K., 2015. Copepods enhance nutritional status, growth and development in Atlantic cod (Gadus morhua L.) larvae-can we identify the underlying factors??. Peer J. 3, e902.

Kimmel, C.B., Miller, C.T., Moens, C.B., 2001. Specification and morphogenesis of the zebrafish larval head skeleton. Dev. Biol. 233, 239–257.

Kleppe, L., Edvardsen, R.B., Furmanek, T., Taranger, G.L., Wargelius, A., 2014. Global transcriptome analysis identifies regulated transcripts and pathways activated during oogenesis and early embryogenesis in atlantic cod. Mol. Reprod. Dev. 81, 619–635.

Lee, A.J., Hodges, S., Eastell, R., 2000. Measurement of osteocalcin. Ann. Clin. Biochem. 37, 432–446.

Lefebvre, V., Bhattaram, P., 2010. Vertebrate Skeletogenesis. Curr. Top. Dev. Biol. 90, 291–317.

Li, H., Durbin, R., 2009. Fast and accurate short read alignment with Burrows-Wheeler transform. Bioinformatics 25, 1754–1760.

Li, H., Handsaker, B., Wysoker, A., Fennell, T., Ruan, J., Homer, N., Marth, G., Abecasis, G., Durbin, R., Proc, G.P.D., 2009. The Sequence Alignment/Map format and SAMtools. Bioinformatics 25, 2078–2079.

Liang, B., Soka, M., Christensen, A.H., Olesen, M.S., Larsen, A.P., Knop, F.K., Wang, F., Nielsen, J.B., Andersen, M.N., Humphreys, D., Mann, S.A., Huttner, I.G., Vandenberg, J.I., Svendsen, J.H., Haunso, S., Preiss, T., Seebohm, G., Olesen, S.P., Schmitt, N., Fatkin, D., 2014. Genetic variation in the two-pore domain potassium channel, TASK-1, may contribute to an atrial substrate for arrhythmogenesis. J. Mol. Cell. Cardiol. 67, 69–76.

Litvin, J., Selim, A.H., Montgomery, M.O., Lehmann, K., Rico, M.C., Devlin, H., Bednarik, D.P., Safadi, F.F., 2004. Expression and function of periostin-isoforms in bone. J. Cell. Biochem. 92, 1044–1061.

Lyons, G.E., 1996. Vertebrate heart development. Curr. Opin. Genet. Dev. 6, 454–460.

Martell, D.J., Kieffer, J.D., Trippel, E.A., 2005. Effects of temperature during early life history on embryonic and larval development and growth in haddock. J. Fish Biol. 66, 1558–1575.

van der Meeren, T., Karlsen, Ø., Liebig, P.J., Mangor-Jensen, A., 2014. Copepod production in a saltwater pond system: a reliable method for achievement of natural prey in start-feeding of marine fish larvae. Aquac. Eng. 62, 17–27.

Merle, B., Bouet, G., Rousseau, J.C., Bertholon, C., Garnero, P., 2014. Periostin and transforming growth factor beta-induced protein (TGF beta Ip) are both expressed by osteoblasts and osteoclasts. Cell. Biol. Int. 38, 398–404.

Minoux, M., Rijli, F.M., 2010. Molecular mechanisms of cranial neural crest cell migration and patterning in craniofacial development. Development 137, 2605–2621.

Misund, O.A., Olsen, E., 2013. Lofoten-Vesterålen: for cod and cod fisheries, but not for oil? ICES J. Mar. Sci. 70, 722–725.

Mitiku, N., Baker, J.C., 2007. Genomic analysis of gastrulation and organogenesis in the mouse. Dev. Cell 13, 897–907.

Mobasheri, A., Shakibaei, M., Marples, D., 2004. Immunohistochemical localization of aquaporin 10 in the apical membranes of the human ileum: a potential pathway for luminal water and small solute absorption. Histochem. Cell Biol. 121, 463–471.

Moksness, E., Kjørsvik, E., Olsen, Y., 2004. Culture of Cold-water Marine Fish. Fishing News Books, Oxford.

Moore, S., Ribes, V., Terriente, J., Wilkinson, D., Relaix, F., Briscoe, J., 2013. Distinct regulatory mechanisms act to establish and maintain Pax3 expression in the developing neural tube. PLoS Genet. 9, e1003811.

Nozawa, Y.I., Lin, C.W., Chuang, P.T., 2013. Hedgehog signaling from the primary cilium to the nucleus: an emerging picture of ciliary localization, trafficking and transduction. Curr. Opin. Genet. Dev. 23, 429–437.

Okada, Y., Naka, K., Kawamura, K., Matsumoto, T., Nakanishi, I., Fujimoto, N., Sato, H., Seiki, M., 1995. Localization of Matrix Metalloproteinase-9 (92-Kilodalton Gelatinase/Type-Iv Collagenase=Gelatinase-B) in Osteoclasts-Implications for Bone-Resorption. Lab. Invest. 72, 311–322.

Olsen, B.R., Reginato, A.M., Wang, W.F., 2000. Bone development. Annu. Rev. Cell Dev. Biol. 16, 191–220.

Olsen, E., Aanes, S., Mehl, S., Holst, J.C., Aglen, A., Gjosaeter, H., 2010. Cod, haddock, saithe, herring, and capelin in the Barents Sea and adjacent waters: a review of the biological value of the area. ICES J. Mar. Sci. 67, 87–101.
Patan, S., 2000. Vasculogenesis and angiogenesis as mechanisms of vascular network formation, growth and remodeling. J. Neuro-Oncol. 50, 1–15.
Ramachandran, K.V., Hennessey, J.A., Barnett, A.S., Yin, X.H., Stadt, H.A., Foster, E., Shah, R.A., Yazawa, M., Dolmetsch, R.E., Kirby, M.L., Pitt, G.S., 2013. Calcium influx through L-type Ca(V)1.2 Ca2+ channels regulates mandibular development. J. Clin. Invest. 123, 1638–1646.
Rosati, B., McKinnon, D., 2004. Regulation of ion channel expression. Circ. Res. 94, 874–883.
Sanguinetti, M.C., Tristani-Firouzi, M., 2006. hERG potassium channels and cardiac arrhythmia. Nature 440, 463–469.
Simoes-Costa, M., Bronner, M.E., 2015. Establishing neural crest identity: a gene regulatory recipe. Development 142, 242–257.
Smith, K.A., Chocron, S., von der Hardt, S., de Pater, E., Soufan, A., Bussmann, J., Schulte-Merker, S., Hammerschmidt, M., Bakkers, J., 2008. Rotation and asymmetric development of the zebrafish heart requires directed migration of cardiac progenitor cells. Dev. Cell 14, 287–297.
Sorhus, E., Edvardsen, R.B., Karlsen, O., Nordtug, T., van der Meeren, T., Thorsen, A., Harman, C., Jentoft, S., Meier, S., 2015. Unexpected interaction with dispersed crude oil droplets drives severe toxicity in atlantic haddock embryos. PLoS One 10, e0124376.
Stainier, D.Y.R., Lee, R.K., Fishman, M.C., 1993. Cardiovascular Development in the Zebrafish. 1. Myocardial Fate Map and Heart Tube Formation. Development 119, 31–40.
Star, B., Nederbragt, A.J., Jentoft, S., Grimholt, U., Malmstrom, M., Gregers, T.F., Rounge, T.B., Paulsen, J., Solbakken, M.H., Sharma, A., Wetten, O.F., Lanzen, A., Winer, R., Knight, J., Vogel, J.H., Aken, B., Andersen, O., Lagesen, K., Tooming-Klunderud, A., Edvardsen, R.B., Tina, K.G., Espelund, M., Nepal, C., Previti, C., Karlsen, B.O., Moum, T., Skage, M., Berg, P.R., Gjoen, T., Kuhl, H., Thorsen, J., Malde, I., Reinhardt, R., Du, L., Johansen, S.D., Searle, S., Lien, S., Nilsen, F., Jonassen, I., Omholt, S.W., Stenseth, N.C., Jakobsen, K.S., 2011. The genome sequence of Atlantic cod reveals a unique immune system. Nature 477, 207–210.
Staudt, D., Stainier, D., 2012. Uncovering the molecular and cellular mechanisms of heart development using the zebrafish. Annu. Rev. Genet. 46, 397–418.
Sumanas, S., Jorniak, T., Lin, S., 2005. Identification of novel vascular endothelial-specific genes by the microarray analysis of the zebrafish cloche mutants. Blood 106, 534–541.
Swartz, M.E., Sheehan-Rooney, K., Dixon, M.J., Eberhart, J.K., 2011. Examination of a Palatogenic Gene Program in Zebrafish. Dev. Dyn. 240, 2204–2220.
Szabo-Rogers, H.L., Smithers, L.E., Yakob, W., Liu, K.J., 2010. New directions in craniofacial morphogenesis. Dev. Biol. 341, 84–94.
Tarazona, S., Garcia-Alcalde, F., Dopazo, J., Ferrer, A., Conesa, A., 2011. Differential expression in RNA-seq: a matter of depth. Genome Res. 21, 2213–2223.
Thisse, B., Pflumio, S., Fürthauer, M., Loppin, B., Heyer, B., Degrave, A., Woehl, R., Lux, A., Steffan, T., Charbonnier, X.Q., Thisse, C., 2001. Expression of the Zebrafish Genome During Embryogenesis https://zfin.org.
Troen, B.R., 2004. The role of cathepsin K in normal bone resorption. Drug News Perspect. 17, 19–28.
Wada, N., Javidan, Y., Nelson, S., Carney, T.J., Kelsh, R.N., Schilling, T.F., 2005. Hedgehog signaling is required for cranial neural crest morphogenesis and chondrogenesis at the midline in the zebrafish skull. Development 132, 3977–3988.
Webb, S.E., Fluck, R.A., Miller, A.L., 2011. Calcium signaling during the early development of medaka and zebrafish. Biochimie 93, 2112–2125.
Yang, H.X., Zhou, Y., Gu, J.L., Xie, S.Y., Xu, Y., Zhu, G.F., Wang, L., Huang, J.Y., Ma, H., Yao, J.H., 2013. Deep mRNA sequencing analysis to capture the transcriptome landscape of zebrafish embryos and larvae. PLoS One, 8.
Zhou, Y., Cashman, T.J., Nevis, K.R., Obregon, P., Carney, S.A., Liu, Y., Gu, A.H., Mosimann, C., Sondalle, S., Peterson, R.E., Heideman, W., Burns, C.E., Burns, C.G., 2011. Latent TGF-beta binding protein 3 identifies a second heart field in zebrafish. Nature 474, 645–648.